Microelectronics Reliability xxx (2016) xxx–xxx

Contents lists available at ScienceDirect

Microelectronics Reliability

journal homepage: www.elsevier.com/locate/microrel

Risk assessment of the crack propagation and delamination of the Cu-to-Cu direct bonded (CuDB) interface

Ah-Young Park [a,*], Satish C. Chaparala [a,b], SeungBae Park [a]

[a] State University of New York at Binghamton, Mechanical Engineering, ITC, 85 Murray Hill Road, 13850 Vestal, NY, United States
[b] Corning Incorporated, 1 Science Center Road, 14870, Erwin, NY, USA

ARTICLE INFO

Article history:
Received 31 December 2015
Received in revised form 13 September 2016
Accepted 24 September 2016
Available online xxxx

Keywords:
Cu-to-Cu direct bonding
Crack
Delamination
Finite element analysis (FEA)
Fracture mechanics
Reliability

ABSTRACT

Through Silicon Via (TSV) technology with micro joint has been identified as the 3D package technology to overcome the limitations of I/O density and enhances the system performance compared to that of the conventional flip chip packages. One of the challenges of the reliable 3D TSV packages is stacking and joining of thin wafers or dies. The conventional micro joining methods, such as use of solder bumps, cause many reliability problems, such as intermetallic compound (IMC) formation, electromigration, delamination, creep, and fatigue problems. As an alternative, copper-to-copper direct bonding (CuDB) has been proposed. CuDB enables reduction in fabrication process steps, can obtain higher interconnect density and enhanced thermal conductivity. However, the CuDB interface has potential reliability risk since the bonding is typically performed by compression at high temperature. Several prior studies have reported formation of small voids between the bonding interfaces of the CuDB that can lead to crack initiation, propagation and thereby delamination of the entire interface. The defect can result in failure of the entire package during its fabrication process or operation.

This study is risk assessment of possibility of crack propagation at the CuDB interface using fracture mechanics approach. Finite element (FE) analysis and design of experiments (DOE) are used. A crack is assigned at the interface of the CuDB to mimic a small void. Initial crack location and dimensional variables (Initial crack length, Cu pad diameter and pitch, and TSV diameter and pitch) are varied to quantify the risk. The strain energy release rate (SERR) around the crack tip is calculated and compared with the critical SERR, obtained by experiments, to judge the possibility of crack propagation. Sensitivity analysis of design parameters is conducted. As a result, this study provides design recommendations that can minimize interfacial failure of the CuDB. In addition, this study explores various numerical modeling methodologies that can be implemented for efficient failure prediction of the interfaces.

1. Introduction

For more than a decade, the Through Silicon Via (TSV) technology has been studied and matured in many directions. This technology offers the shortest vertical interconnection with stacked chips [1,2]. Various interconnection methods are available with the TSV, such as the conventional micro bump with the solder and underfill, wire-bonding, and Cu-to-Cu direct bonding. The conventional solder-based interconnection has been widely used in electronic device applications. The interconnection is enable to obtain finer and higher density interconnection with lower reliability risk. However, the solder-based interconnection can be applied to low power consumption application due to the low effective thermal conductivity. Moreover, several reliability issues, such as intermetallic compound (IMC) formation, electromigration, creep, fatigue problems and thermal management of the 3D package arises and still need to be addressed.

Alternative interconnection technology is the copper-to-copper direct bond (CuDB). Fig. 1 shows a bonded wafer by the CuDB [3]. CuDB has many advantages over the conventional solder joint technology. CuDB technology eliminates the need for process steps, such as UBM deposition, lithography, and electroplating, thus, significant time and cost savings can be realized. Copper has better thermal conductivity than that of the solder, enabling lower junction temperature. Intermetallic compounds (IMC) problem, which is a serious issue of the conventional solder-based interconnection, is no longer relevant [4].

As illustrated in Fig. 2, high bonding temperature (250–400 °C) and pressing force are required for the thermal-compression bonding [5,6]. It is one of potential problems of the CuDB, since it may damage fabricated electrodes and bumps. Another issue is void formation at the CuDB interface due to the surface roughness. Several prior studies [7–10] have reported void formation at the bonded interface of the CuDB as shown in Fig. 3 [9,10]. The small void can act as an initial crack and

* Corresponding author.
E-mail address: apark10@binghamton.edu (A.-Y. Park).

http://dx.doi.org/10.1016/j.microrel.2016.09.015
0026-2714/

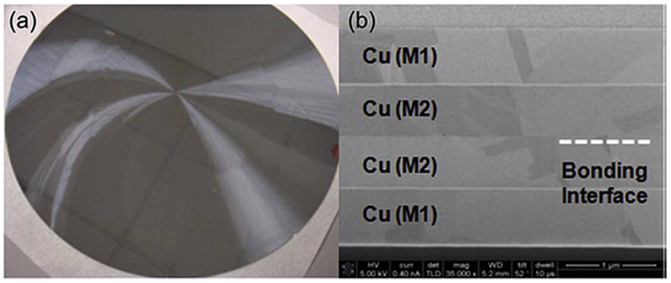

Fig. 1. (a) Bonded wafer pair with the top donor wafer successfully ground back to 100 μm, showing that Cu-to-Cu bonding is sufficiently strong to sustain mechanical grinding. (b) Cross-sectional view of properly bonded wafers [3].

can eventually propagate. Delamination can occur in the board level reflow or thermal cycling due to the thermal expansion coefficient (CTE) mismatch between a substrate and stacked chips [11,12]. Fig. 4 presents an example of delamination between Cu landing pads (M1) and TSV Cu nails [12].

This study is to assess the possibility of crack propagation at the CuDB. Finite element (FE) analysis and design of experiments (DOE) are used. In addition, sensitivity analysis of design parameters is conducted. Numerical analysis at around the crack during temperature change is performed using a commercially available finite element software, ANSYS™. Submodeling technique is adopted to simulate the region of interest multi-scale geometries of the package. A DOE-based parametric study has been conducted to determine the impact of the initial crack location and geometry variables, such as initial crack length, Cu pad diameter and pitch, and TSV diameter and pitch. Furthermore, the strain energy release rate (SERR) has been calculated from the stress intensity factor (SIF) at the crack tip. The SERR calculations are verified by the J-integral method. The estimated SERR's are compared with the critical SERR (fracture toughness of this interface), which is obtained by experiments, to determine the risk of crack propagation. Fracture toughness values are obtained from other research studies [13,20–24]. A thermal load [14] simulating a cooling process is used in this study as shown in Fig. 5. Three different types of simple geometries of 2D and 3D through thickness crack models are tested. As the most conservative result, a 2D half-symmetry model with the plane strain condition under the isothermal loading is used in this paper.

2. Finite element modeling

A 3D package comprising a substrate, C4 and underfill layer, stacked silicon dies with CuDB and an intermediate layer is modeled. The top silicon die is 150 μm and the bottom silicon die is thinned to 50 μm. The intermediate layer between the two dies is assumed to be SiO_2, which is widely used for the CuDB. Each Cu pad dimension is 3 μm tall, 7.5 μm diameter and 10 μm pitch. A cross-section view of the package is shown in Fig. 6. Details of the package dimensions are summarized in Table 1. These dimensions are extracted from the experimental data in authors' previous study which presented the design of a TSV and CuDB chip-package interaction test vehicle and first reliability results of the TSV/CuDB combined interconnect [13].

In the geometry analyzed, the substrate and dies have millimeter length scales while the CuDBs and TSVs have micrometer length scales. Therefore, the submodeling is used to accurately model the stress state in the interface of CuDB. FE simulation starts from a global model of the entire package with a relatively coarse mesh to get accurate displacement results. The displacement results will be transferred to a submodel as boundary conditions at the cut boundary interface to capture the detail behavior in the zoomed up model.

For more detail behavior of the region of interest, the outermost TSV and CuDB are selected because they are identified as the highest risk of failure. The submodel consists of the outermost TSV and CuDB with a SiO_2 intermediate layer, substrate, solder ball, and two dies. Fig. 8 shows a schematic of the submodel of the region in which the bump dimensions are 10 μm wide and 1286 μm tall. This study assumes that there is a pre-existing crack at the bonded interface of the CuDB. Contact interaction is enforced on the two crack faces of the initial crack as illustrated in Fig. 6(b).

A snap shot of the global and submodel is shown in Fig. 7. The global model has no individual TSVs and Cu pads due to the scale difference. Instead, the effect of these small-scale structures is taken into account as layers with effective material properties. The effective properties may be calculated using an effective Young's modulus and effective CTE equation [15]. The relationship used to calculate the effective material properties are given below. The effective properties are varied by area fraction of copper in a unit cell.

In-plane (x and y) effective Young's modulus, $E^{eff}_{x,y}$:

$$E^{eff}_{x,y} = \frac{1}{\left[\frac{c_{cu}}{E_{cu}} + \frac{c_s}{E_s}\right] - \frac{c_{cu}c_s(\nu_s E_{cu} - \nu_{cu}E_s)^2}{E_{cu}E_s(c_{cu}E_{cu} + c_s E_s)}} \quad (1)$$

Out-of-plane (z) effective Young's modulus, E^{eff}_z:

$$E^{eff}_z = c_{cu}E_{cu} + c_s E_s \quad (2)$$

Out-of-plane effective Poisson's ratio, ν^{eff}_{xz}:

$$\nu^{eff}_{xz} = c_{cu}\nu_{cu} + c_s\nu_s \quad (3)$$

In-plane effective CTE, $\alpha^{eff}_{x,y}$:

$$\alpha^{eff}_{x,y} = (1+\nu_{cu})\alpha_{cu}c_{cu} + (1+\nu_s)\alpha_s c_s - \alpha^{eff}_z \nu^{eff}_{xz}, \quad (4)$$

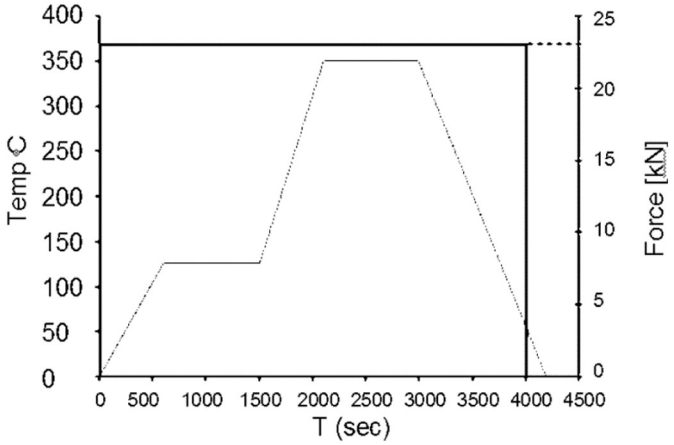

Fig. 2. Typical bonding profile used for wafer to wafer [5,6].

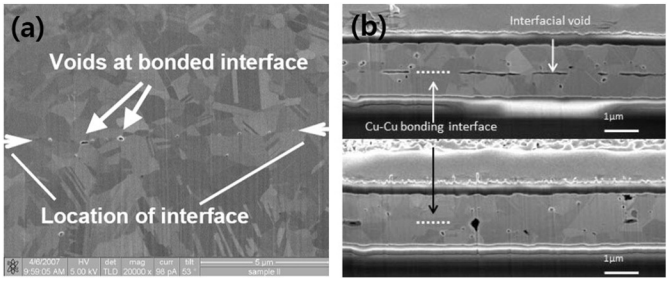

Fig. 3. FIB cross-section of Cu—Cu thermo-compression bump (a) 20 μm bumps bonded at 300 °C. (b) Cu—Cu bond at adjacent Kelvin structures without Cu seal ring (top) and (b) with Cu seal ring (bottom). Interfacial voids are presented at the bonded interface [9,10].

Please cite this article as: A.-Y. Park, et al., Risk assessment of the crack propagation and delamination of the Cu-to-Cu direct bonded (CuDB) interface, Microelectronics Reliability (2016), http://dx.doi.org/10.1016/j.microrel.2016.09.015

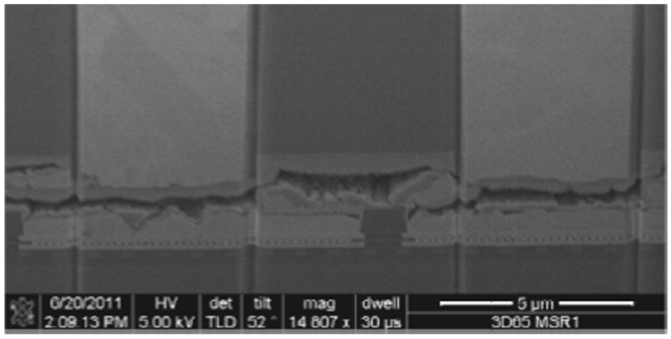

Fig. 4. Landing pads delaminate and stick to the top die of TSV Cu nails due to pull back effect coming from the warpage of thin die [12].

where ν is the Poisson's ratio and c is area fraction. Subscript cu is Copper for TSV and Cu pad, and s is Silicon and SiO_2, respectively.

The constitutive model of copper at the size scale of interest in this study is elastic-plastic stress-strain relation with bilinear isotropic hardening. All other materials are assumed to be linear elastic. Table 2 provides the material properties of the materials including plastic properties of copper [25] considered in this study.

Three different types of simple geometries of 2D and 3D through thickness crack models are tested to compare results depending on assumptions and used element types. For the simplicity, a symmetric condition is applied at the center of the half section of the model, and all degrees of freedom of the bottom points are fixed to prevent rigid body motion. For the 2D model, quadratic solid element Plane183 is used with plane strain condition. Solid185 and Solid186 elements are used for the 3D surface crack model. As the most conservative result, the 2D half-symmetry model with the plane strain condition under the isothermal loading is used in following parametric study.

Reference temperature where the package is assumed to be strain free is 125 °C. The final temperature which the package is cooled down is 25 °C. Isothermal loading is assumed. As stated in K.H. Lu [14], a positive thermal load ($\Delta T = T_{RT} - T_{Ref} > 0$) subjects the interfacial crack to only pure shear. A negative thermal load ($\Delta T = T_{RT} - T_{Ref} < 0$) subjects the interfacial crack to both normal and shear forces. Therefore, the negative thermal load leads delamination at the interface. Since both normal and shear stresses exist at the crack, the crack propagation could be accelerated once it starts to propagate.

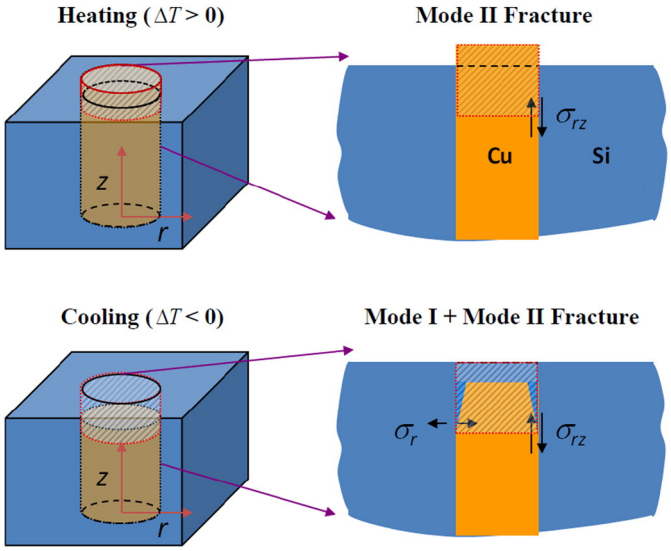

Fig. 5. Schematics of interfacial delamination of TSV under cooling and heating conditions. In both cases, the interfacial crack is assumed to grow asymmetrically from one surface towards the other surface.

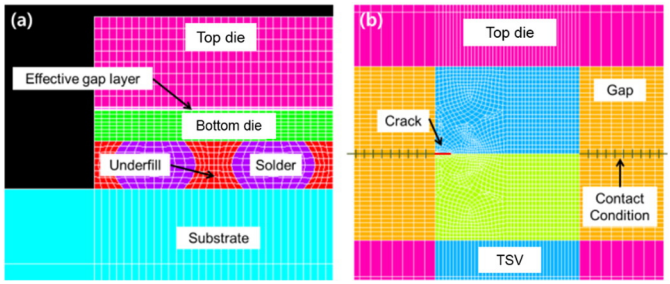

Fig. 6. (a) Finite-element mesh of the global model. (b) Finite-mesh of the submodel with the left side crack.

The effect of crack location on the stress and strain energy release rate (SERR) is investigated. Cracks are placed in three different places within the CuDB. Twenty different cases of the global model and sixty different cases of submodel are analyzed the effects of initial crack length, Cu pad diameter/pitch and TSV diameter, and pitch. The strain energy release rates (SERRs) are calculated from the stress intensity factors and the values obtained are further verified with those obtained using the J-integral. The SERRs are compared with the critical SERR (Fracture toughness) to predict the possibility of crack propagation.

3. Result and discussion

The displacement boundary conditions in the submodel are obtained by solving the global model. It needs to be verified if these boundary conditions are accurately transferred from the global model to the submodel. As shown in Fig. 9, the selected node 1738, 234, and 122 in the global model correspond to the node 49,043, 802, and 842 in the submodel, respectively. The displacement in y-direction is 15.289 µm for the nodes 1738 and 49,043. Similarly, the displacement of nodes 234 and 802 is 14.977 µm, and that of nodes 122 and 842 is 12.738 µm. This confirms that the three values of displacement from the global model are accurately transferred as boundary conditions into the submodel.

3.1. Different type of 2D and 3D through thickness crack models

Analytical solutions of a single-edge crack are well known as stated in Fig. 10 [26], however, they can be varied depending on modeling assumptions and used element types in FE analysis. Therefore, three different types of simple geometries of 2D and 3D through thickness crack models are tested to find an appropriate simulation method in modeling perspective. Only a surface crack through thickness is considered in this study. If a penny crack needs to be considered, additional simulations are required. However, a penny crack has much smaller SIF compared with that of the through thickness crack according to analytic solutions. For the 2D model, quadratic solid element Plane183 (eight nodes per each element) is used with plane strain condition. Solid185 (eight node per element) and Solid186 (twenty nodes per element) elements are used for the 3D surface crack model.

Edge crack (a/b = 1/4) in a finite plate under uniaxial stress is chosen because in-plane tension is dominant at the crack of the outermost

Table 1
Geometry details.

Item	Dimension
Substrate	24 mm (L) × 1 mm (T)
Top silicon die	8 mm (L) × 0.15 mm (T)
Bottom silicon die	8 mm (L) × 0.05 mm (T)
Solder ball	100 µm (D) / 200 µm (P) / 80 µm (H)
TSV	5 µm (D) / 10 µm (P)/50 µm (H)
Cu micro-bump	7.5 µm (D) / 10 µm (P) / 3 µm (H)

(L, length; T, thickness; D, diameter; P, pitch; H, height).

Please cite this article as: A.-Y. Park, et al., Risk assessment of the crack propagation and delamination of the Cu-to-Cu direct bonded (CuDB) interface, Microelectronics Reliability (2016), http://dx.doi.org/10.1016/j.microrel.2016.09.015

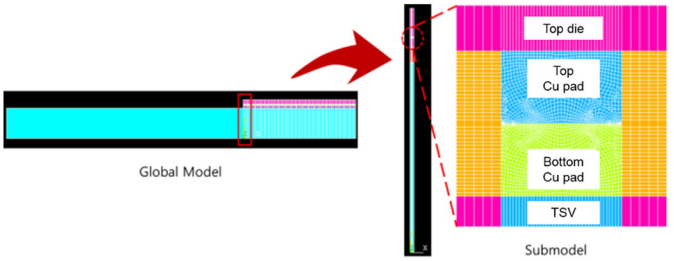

Fig. 7. Schematics of Submodeling method.

CuDB according to the previous study [4,19]. Ratio of simulated $K_{I,simulation}$ to Analytic solution K_I is calculated for each case; $K_{I,simulation}/K_I$ of 2D model = 0.996, $K_{I,simulation}/K_I$ of 3D model using Solid185 = 0.937, and $K_{I,simulation}/K_I$ of 3D model using Solid186 = 0.936. This result indicates that the 2D model is the most conservative to predict the SIF. According to a comparison study between 2D and 3D crack analysis with a surface crack through thickness, the in-plane stresses are nearly constant through the thickness with the normal stresses dropping off by approximately 25% at the free surface. In addition, the out-of-plane stress in the center of the plate, very close to the crack tip, is plane strain. Thus the 2D stress fields provide and accurate description of the 3D problem [27,28]. Therefore, the 2D model is used in following study.

3.2. Critical location in the CuDB with a pre-existing crack

To obtain critical location of the crack, three different locations of the cracks are analyzed as shown in Fig. 11(a)–(c). All of cases have the same length of crack at the interface, which is 0.5 μm. It may be expressed that 0.5 μm is equal to the crack length 2*a* for the case of a center crack and crack length *a* for the case of an edge crack in Fig. 10. Minimum mesh size is 0.0625 μm near the crack tip in the submodel

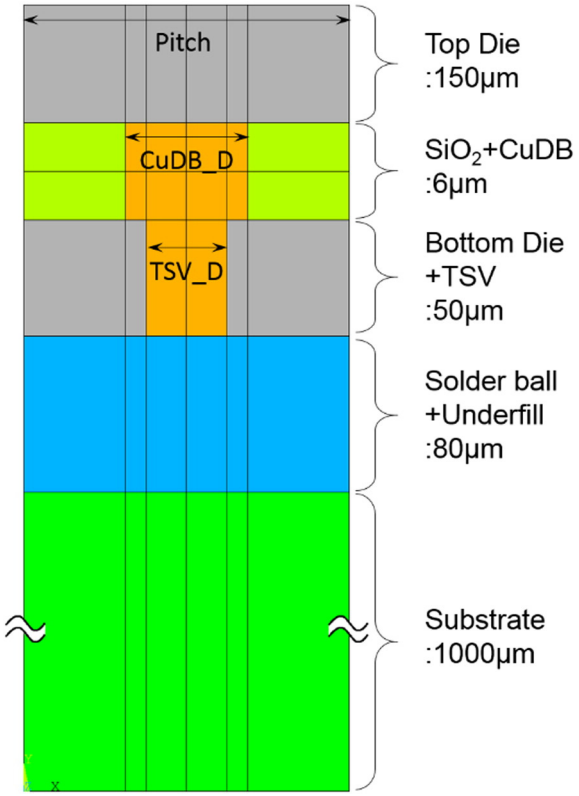

Fig. 8. Schematic of the unit cell of the submodel.

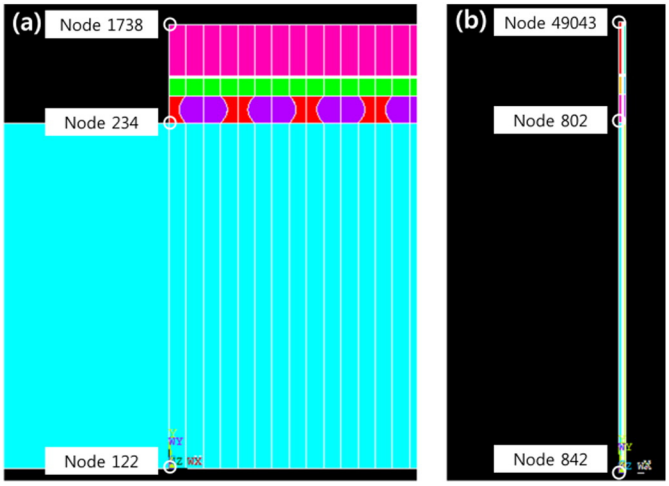

Fig. 9. Selected nodes for verification of the submodeling.

because singular elements around the crack tip should have a radius of approximately less than one eighth of the crack length [17]. Fig. 11 shows stress distribution of the CuDB. Average stress inside of the CuDB is less than the yield strength of the copper. Especially, Fig. 11(d) and (e) show stress distribution of the left pre-crack case depending on mesh size of 0.0625 μm and 0.0125 μm, respectively. Strain energy release rates (SERR) G are calculated to compare with the critical SERR G_c. The SERR of the each case is obtained from the relation of the stress intensity factor K, displacement, and the crack length at and near the crack [18].

Fig. 12 shows the calculated SERRs for the cases of mode I, mode II and the mixed loading. It is observed that in-plane tension is dominant than in-plane shear for all cases; G_I^L (mode I of the left pre-crack case) = 0.538 (J/m^2), G_I^R (mode I of the right pre-crack case) = 0.448 (J/m^2), G_I^C (mode I of the center pre-crack case) = 0.287 (J/m^2), while $G_{II}^L = 0.0236$ (J/m^2), $G_{II}^R = 0.0059$ (J/m^2), $G_{II}^C = 0.0001$ (J/m^2). This result indicates that in-plane tension plays a crucial role in crack propagation. The CuDB is held between silicon dies which can reduce warpage locally rather than substrate-silicon combination. The warpage causes in-plane tension in the outermost CuDB. As a result, failure can occur by in-plane tension near the crack tip.

The J-integral is used to predict the SERR values and are compared with the values obtained from stress intensity factors. The calculated results are listed in Table 3. Strain energy release rate values estimated

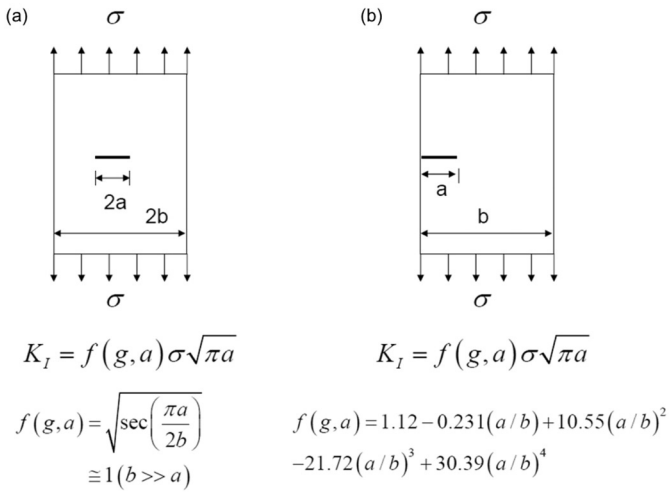

$$K_I = f(g,a)\sigma\sqrt{\pi a}$$

$$f(g,a) = \sqrt{\sec\left(\frac{\pi a}{2b}\right)} \cong 1 \quad (b >> a)$$

$$K_I = f(g,a)\sigma\sqrt{\pi a}$$

$$f(g,a) = 1.12 - 0.231(a/b) + 10.55(a/b)^2 - 21.72(a/b)^3 + 30.39(a/b)^4$$

Fig. 10. Analytic solutions of Stress intensity factors of (a) a center-crack with crack length denoted as 2*a* and (b) an edge-crack with crack length *a* [26].

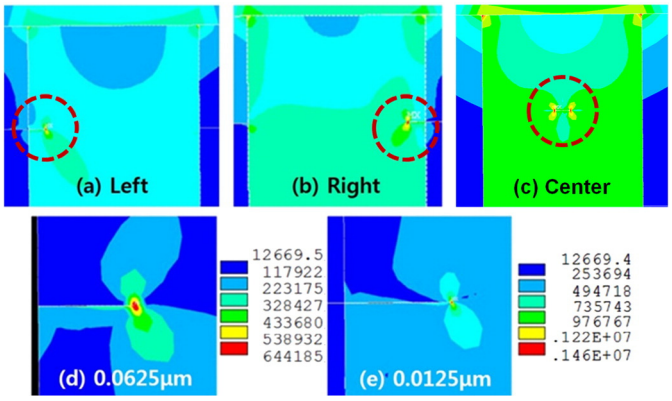

Fig. 11. Equivalent stress distribution of (a) Left crack (b) Right crack, and (c) Center crack. Zoomed crack area of the left pre-crack with (d) mesh size 0.0625 μm, and (e) mesh size 0.0125 μm. Units are kPascals.

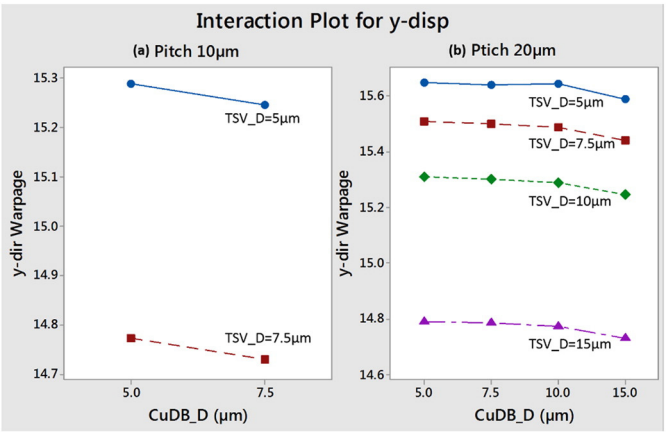

Fig. 13. Warpage results of the entire package depending on the parameters (a) 10 μm pitch (b) 20 μm pitch.

from the above mentioned two approaches agree very well. According to the SERR calculation, the case of left pre-crack has the highest total G value. Besides, it shows the highest G_{II} value, which affects on crack propagation and accelerates the failure once it starts to propagate due to existence of both normal and shear stresses. Therefore, the case of the left pre-crack is selected for following analysis.

3.3. Warpage results of the global model

A DOE-based parametric study is adopted for sensitivity analysis of package geometry parameters, such as initial crack length, Cu bumps diameter and pitch, and TSV diameter and pitch. FE analysis and design of experiments (DOE) is used. The parameter matrix is listed in Table 4. Twenty different cases are analyzed using the global model described earlier. The outermost point at the interface of the effective intermediate layer of SiO_2 and a Cu bump is chosen to measure the displacements.

The package is warped about 14 μm–16 μm depending on the effective modulus of the TSV and CuDB layer. The magnitude of the predicted warpage is 2% of the diagonal length of the package, which is acceptable from manufacturing and quality considerations. Warpage decreases as the pitch decreases, TSV diameter increases, and CuDB increases, respectively, as shown in Fig. 13. The results are highly related with the corresponding copper area fraction of the effective layers. The increase of copper area fraction directly affects to a CTE increase and Young's modulus decrease. Thus, the CTE difference between the effective layers and the substrate decreases. It results in less displacements under the same loading, since the substrate is dominantly occupied in the package. It is noticed that area fraction of the copper is the main parameter to determine the warpage. Even if parameters of the TSV and CuDB pitch and diameter are different, predicted displacements are the same when the cases have the same copper area fraction. For example, in Fig. 13, the cases of 19.6% copper area fraction, such as (20 μm pitch, 10 μm diameter) and (10 μm pitch, 5 μm diameter), show the same y-direction displacement.

Fig. 14 shows the main effects plots of the warpage on x-displacement and y-displacement, respectively, depending on the parameters of the TSV and CuDB diameter. From this figure, the CuDB diameter has a negligible effect because of its thickness of 6 μm. Compared with that of the TSV layer of 80 μm, it is <10%. It is too thin to affect to the entire package, which is about 1 mm thickness. Therefore, the CuDB variation affects negligibly on the warpage.

3.4. Strain energy release rate calculation for parametric study

A total of 60 cases are simulated to investigate the risk of crack propagation using strain energy release rate calculations. Displacements in x-direction are much smaller than those of in the y-direction in the package. Therefore, in-plane tension is dominant in the outermost CuDB. Thus, failure can occur by in-plane tension near the crack tip, not by in-plane shear.

Fig. 15 presents the main effects plot for G_{total}. Here, the effect plots of the TSV diameter, CuDB diameter, and crack length are extracted from the case of 20 μm pitch, since diameter of the TSV and CuDB cannot exceed 10 μm in the case of 10 μm pitch. In Fig. 15, G_{total} tends to increase as the pitch increases, TSV diameter increases, CuDB diameter

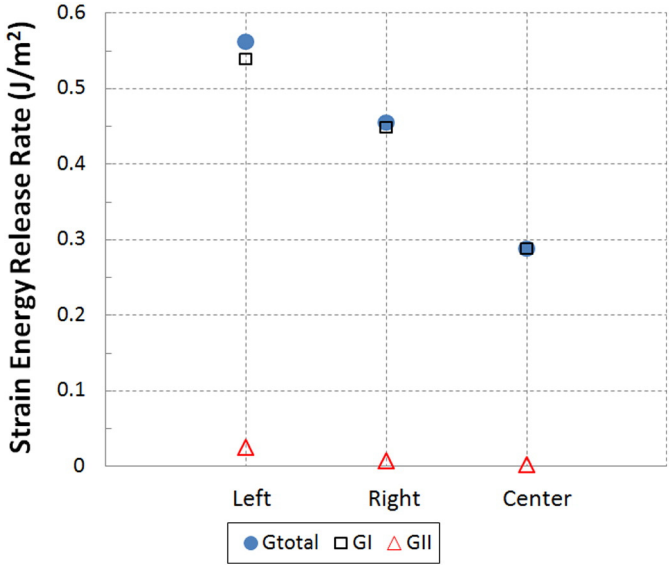

Fig. 12. Strain energy release rates for each case.

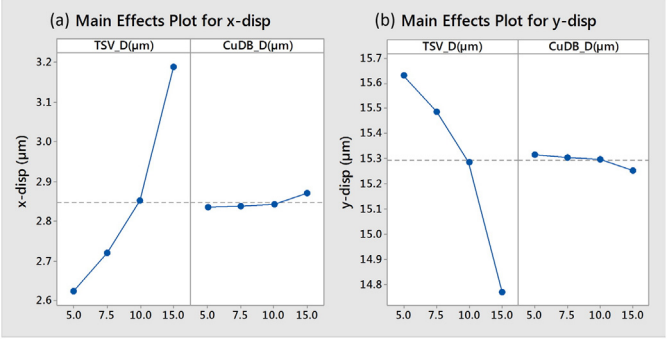

Fig. 14. Main effects plot of the (a) x-displacement and (b) y-displacement in the 20 μm pitch.

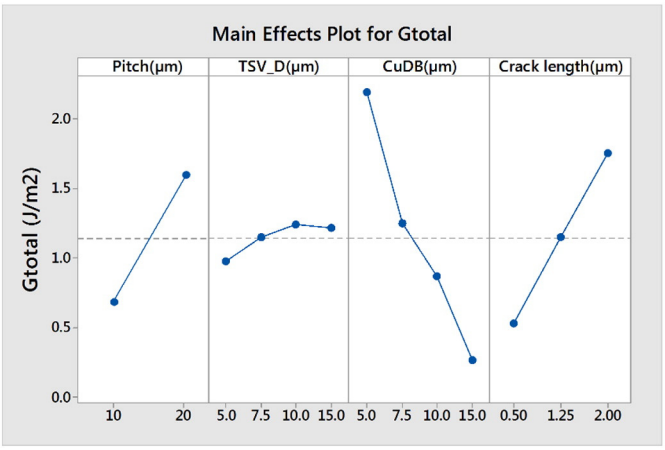

Fig. 15. Main effects plot for Gtotal.

decreases, and crack length increases, respectively. Contrary to the warpage, TSV diameter has less interaction to the SERR at the crack tip, but, the CuDB diameter plays an important role on the SERR. The SERR is affected by neighboring stress of the crack tip. Consequently, the TSV diameter can be a negligible parameter in the calculation of the SERR. The SERR is not directly proportional to the TSV diameter.

Fig. 16 shows the main effects plots of the parameters on the G_I and G_{II} in the model with 20 μm pitch. In-plane tension, represented by the G_I value, is a crucial factor in crack propagation. Fig. 15(a) depicts the same trend as shown in Fig. 15. The increase of the TSV diameter does not appear to impact G_I as shown in the Fig. 16(a). G_I slightly decreases in the case of the 15 μm TSV diameter due to a sharp decrease of warpage from 10 μm to 15 μm of the TSV diameter while it increases in all other cases. The result shows that the SERR decreases as the CuDB diameter increases. It is highly related with the corresponding area fraction of the CuDB. As the CuDB diameter increases, bonding force between two dies becomes stronger due to the increase of the CuDB area fraction, which supports to hold the top die [19]. Therefore, relatively low in-plane tension and in-plane shear concentrate locally at the outermost CuDB, and therefore low SERR can be obtained as shown in Fig. 15.

The SERR decreases, as the CuDB diameter increases, the crack length decreases, and the pitch decreases. It is noted that the effect of the crack length can be changed when the length of pre-crack increases at the interface. An interaction plot among the parameters is shown in Fig. 17. Fig. 18 presents the SERR results depending on the parameters. Additionally, the J-integral is applied to verify the SERR values, and they are highly correlated with about 2% error.

According to several research papers about experiments of the interfacial adhesion energy of the CuDB [13,20–22], the critical strain energy release rate G_c is measured to be between 2.8–15 J/m^2 depending on the CuDB neighboring structure thickness, surface treatment prior to bonding, and post-annealing condition. The interfacial adhesion energy is

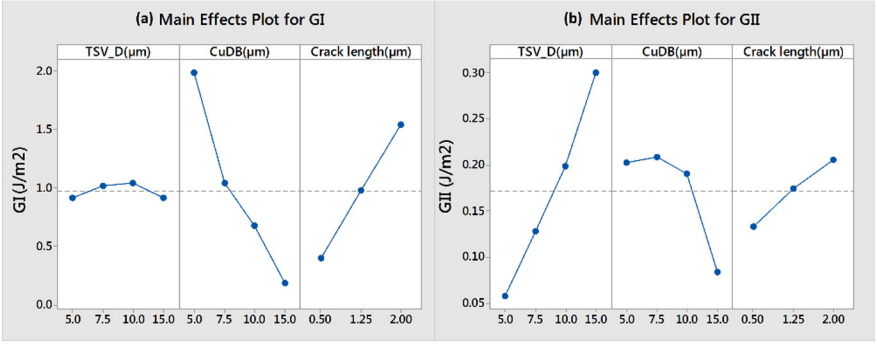

Fig. 16. Main effects plot for (a) GI and (b) GII in the 20 μm pitch.

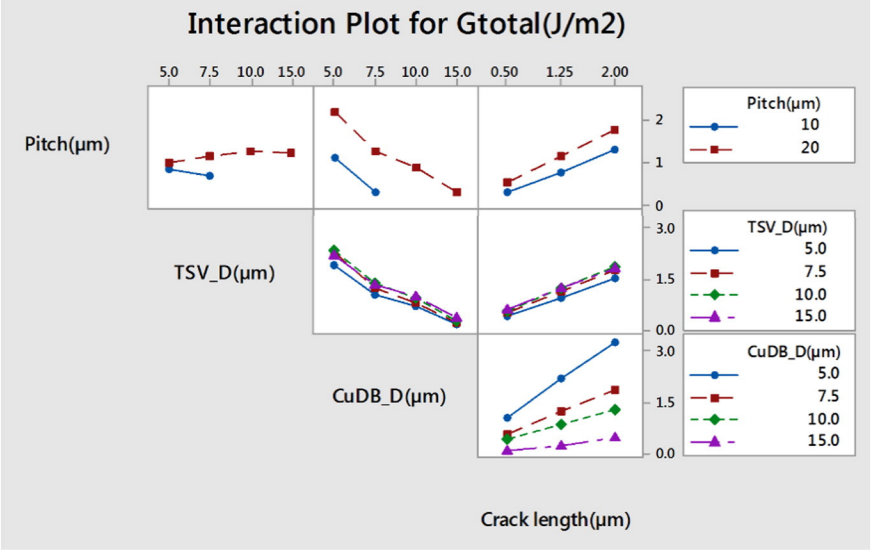

Fig. 17. Interaction plot for G_{total}.

Please cite this article as: A.-Y. Park, et al., Risk assessment of the crack propagation and delamination of the Cu-to-Cu direct bonded (CuDB) interface, Microelectronics Reliability (2016), http://dx.doi.org/10.1016/j.microrel.2016.09.015

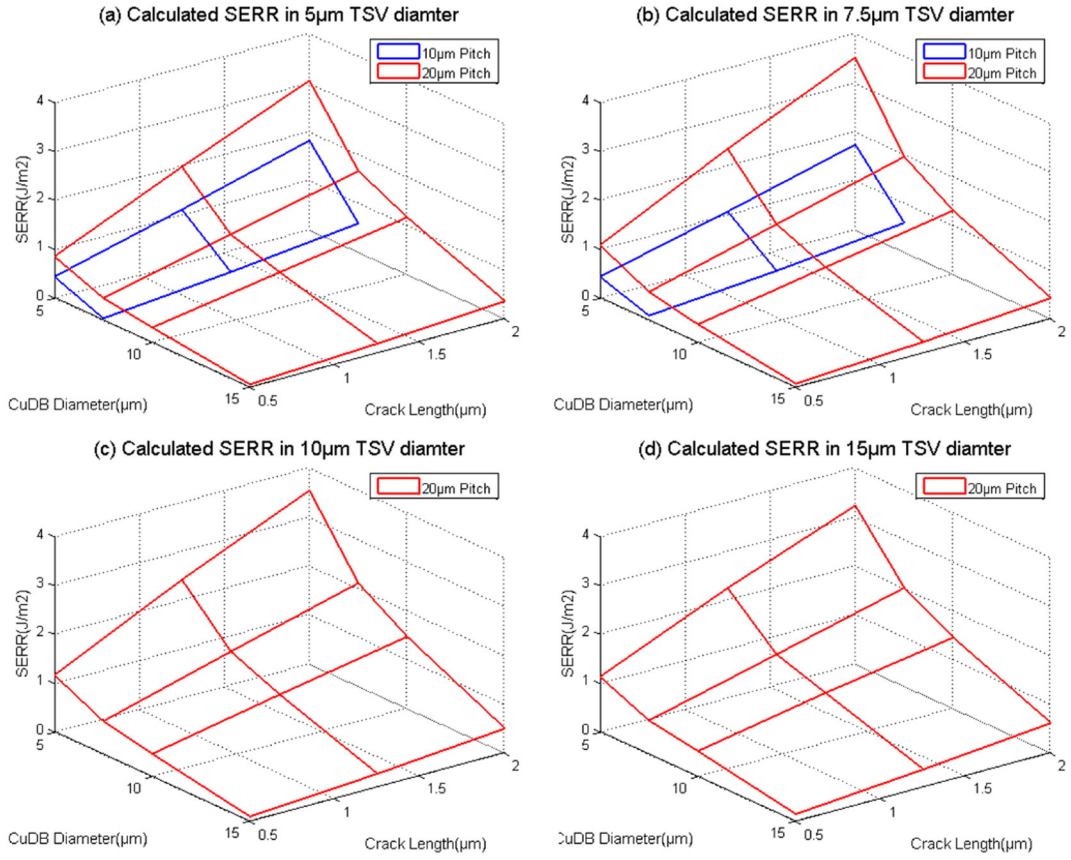

Fig. 18. Calculated SERR depending on CuDB diameter and initial crack length in (a) 5 μm TSV diameter (b) 7.5 μm TSV diameter (c) 10 μm TSV diameter, and (d) 15 μm TSV diameter.

2.8–5.0 J/m^2 depending on bonding temperature, and it can be increased up to 12 J/m^2 when post-annealing is conducted. M. C. Hsieh [23,24] chose 7–10 J/m^2 as the critical SERR. A result with the same dimension of this study shows 8.5–0.3 J/m^2 of the critical adhesion energy at the Cu-SiO_2 interface and not at the CuDB interface as shown in Fig. 19 [13]. Thus, the actual CuDB bond strengths are even higher than the result. As shown in Table 5, the cases which have 5 μm CuDB diameter and 2 μm initial crack length in this simulation, obtain high risk of crack propagation, compared with the minimum critical SERR of 2.8 J/m^2. In addition, the cases of 5 μm CuDB diameter and 1.25 μm initial crack length also present high SERR values, which are close to the critical SERR, regardless of the TSV diameter and pitch.

From these results, large diameter of the CuDB, small pitch of the TSV&CuDB, and small length of the crack recommended to avoid crack propagation. Among analyzed cases in this study, the case of 7.5 μm diameter of the CuDB, 10 μm pitch of the TSV&CuDB, and 0.5 μm length of the crack shows the least risk of crack propagation. Change of the TSV diameter does not appear to impact G_I. An increase of area fraction of the TSV and CuDB, which is determined by the ratio of copper and silicon, is a crucial factor to reduce warpage of the entire package and possibility of crack propagation. Voids of 0.5–1.25 μm length, at the interface during the thermo-compressive bonding process, are acceptable without risk of crack propagation and delamination.

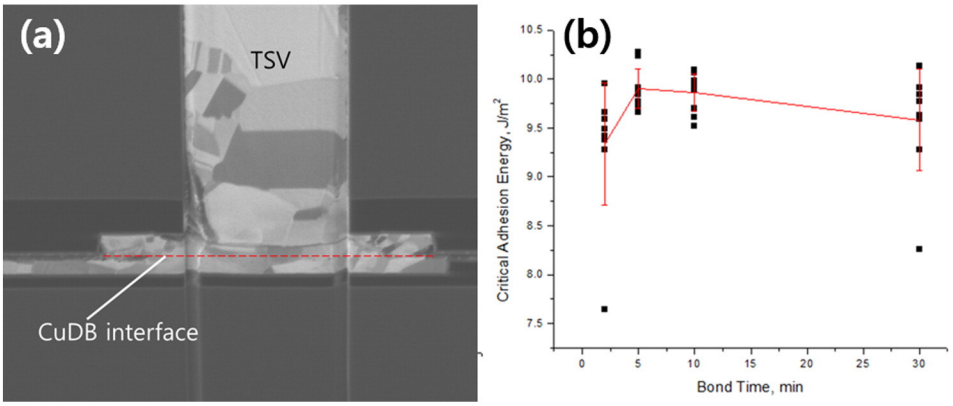

Fig. 19. (a) CuDB interface with TSV, (b) 4-point bend bond strength vs. bonding time for a CuDB [13].

Please cite this article as: A.-Y. Park, et al., Risk assessment of the crack propagation and delamination of the Cu-to-Cu direct bonded (CuDB) interface, Microelectronics Reliability (2016), http://dx.doi.org/10.1016/j.microrel.2016.09.015

Table 2
Effective properties and actual properties for modeling.

	Young's modulus (GPa)	CTE (ppm/°C)	Poisson's ratio
Substrate	23 (below Tg) 13 (above Tg)	16	0.3
Solder ball	50.7 (25 °C) 45.4 (95 °C) 42.8 (130 °C) 34.2 (245 °C)	21.5	0.4
Underfill	5.07 (below Tg) 0.09 (above Tg)	45 143	0.33 0.48
Copper	128.9 240 @ 0 ε 250 @ 0.003 ε 255 @ 0.007 ε 255 @ 0.009 ε	17	0.34
Silicon [16]	169 (x) 169 (y) 130 (z)	3	0.064 (xy) 0.36 (yz) 0.28 (zx)
SiO_2	70	0.55	0.17

Table 3
G_{total}, J values and errors for each case.

Case	G_{total} (J/m^2)	J	Error (%)
Left crack	0.5616	0.5565	0.916
Right crack	0.4535	0.4519	0.354
Center crack	0.2871	0.2857	0.490

Table 4
Matrix of parametric study.

Pitch	TSV diameter	CuDB diameter	Initial crack length
10 μm	5 μm	5 μm	0.5 μm
20 μm	7.5 μm	7.5 μm	1.25 μm
	10 μm	10 μm	2.0 μm
	15 μm	15 μm	

4. Conclusions

In this paper, failure risk optimization of the CuDB interface with a pre-existing crack is numerically investigated. Effects of the crack location and package geometry parameters on crack propagation are analyzed. As the most conservative method, a 2D half-symmetry model with the plane strain condition under the isothermal loading is used. Submodeling technique is applied to analyze multi-scale package warpage, and the strain energy release rates are calculated. The calculated SERRs are compared with the critical SERR to determine if the pre-existing crack can propagate. In addition, sensitivity analysis of design parameters is conducted.

In-plane tension results in higher strain energy release rates at the crack tip compared with the cases of in-plane shear. The highest G_I value is predicted to be at outermost crack tip with $G_I^L = 0.538$ (J/m^2). Area fraction of the copper in the unit cell is the most important factor that affects the warpage of the package. The SERR decreases as the CuDB diameter increases, the crack length decreases, and the pitch decreases. The CuDB diameter is the dominant factor that affects the SERR at the crack tip, followed by the initial crack length and the pitch. Most of the cases of 5 μm CuDB diameter show the high SERR value. Especially, the cases with 1.25 μm and 2 μm initial crack length exceed the critical SERR and under risk of crack propagation. Large diameter of the CuDB is recommended to reduce possibility of crack propagation and delamination at the crack tip. The case of 7.5 μm diameter of the CuDB, 10 μm pitch of the TSV&CuDB, and 0.5 μm length of the crack shows the least risk of crack propagation in this study. Voids of 0.5–1.25 μm length, formed at the interface during the thermo-compressive bonding process, are acceptable and do not pose the risk of crack propagation and delamination.

Table 5
6 cases of the highest G_{total}.

Pitch (μm)	TSV_D (μm)	CuDB_D (μm)	Crack length (μm)	G_I (J/m^2)	G_{II} (J/m^2)	G_{total} (J/m^2)	J-value (J/m^2)	Error (%)
20	10	5	2	3.29	0.23	3.52	3.58	1.88
20	7.5	5	2	3.34	0.15	3.49	3.56	1.84
20	15	5	2	2.76	0.44	3.21	3.27	1.92
20	5	5	2	2.96	0.06	3.02	3.08	1.82
20	10	5	1.25	2.17	0.23	2.39	2.44	1.80
20	7.5	5	1.25	2.18	0.15	2.33	2.37	1.75

References

[1] U. Kang, H.J. Chung, S. Heo, D.H. Park, H. Lee, J.H. Kim, S.H. Ahn, S.H. Cha, J. Ahn, D.M. Kwon, 8 Gb 3-D DDR3 DRAM using through-silicon-via technology, IEEE J. Solid State Circuits 45 (1) (2010) 111–119.
[2] A. Topol, D.C.L. Tulipe, L. Shi, D. Frank, K. Bernstein, S. Steen, A. Kumar, G. Singco, A. Young, K. Guarini, Three-dimensional integrated circuits, IBM J. Res. Dev. 50 (4.5) (2006) 491–506.
[3] C.S. Tan, L. Peng, J. Fan, H. Li, S. Gao, Three-dimensional wafer stacking using Cu—Cu bonding for simultaneous formation of electrical, mechanical, and hermetic bonds, IEEE Trans. Device Mater. Reliab. 12 (2) (2012) 194–200.
[4] A.Y. Park, S. Chapalara, S.B. Park, A fracture mechanics based parametric study of the copper-to-copper direct thermo-compression bonded interface using finite element method, In ASME 2013 International Technical Conference and Exhibition on Packaging and Integration of Electronic and Photonic Microsystems, American Society of Mechanical Engineers, 2013 (pp. V001T01A006).
[5] C. Huyghebaert, J. Van Olmen, Y. Civale, A. Phommahaxay, A. Jourdain, S. Sood, S. Farrens, P. Soussan, Cu to Cu interconnect using 3D-TSV and wafer to wafer thermocompression bonding, Interconnect Technology Conference (IITC), International, IEEE 2010, pp. 1–3.
[6] K. Chen, C. Tan, A. Fan, R. Reif, Copper bonded layers analysis and effects of copper surface conditions on bonding quality for three-dimensional integration, J. Electron. Mater. 34 (12) (2005) 1464–1467.
[7] Y.S. Tang, Y.J. Chang, K.N. Chen, Wafer-level Cu—Cu bonding technology, Microelectron. Reliab. 52 (no. 2) (2012) 312–320.
[8] R.I. Made, P. Lan, H.Y. Li, C.L. Gan, C.S. Tan, Effect of direct current stressing to Cu—Cu bond interface imperfection for three dimensional integrated circuits, Microelectron. Eng. 106 (2013) 149–154.
[9] W. Ruythooren, A. Beltran, R. Labie, Cu—Cu bonding alternative to solder based micro-bumping, Electronics Packaging Technology Conference, IEEE 2007, pp. 315–318 EPTC 2007 9th.
[10] L. Peng, L. Zhang, H. Li, C.S. Tan, Cu—Cu bond quality enhancement through the inclusion of a hermetic seal for 3-D IC, IEEE Trans. Electron Devices 60 (4) (2013) 1444–1450.
[11] Y. Hu, C. Liu, M. Lii, K. Rebibis, A. Jourdain, A.L. Manna, G. Beyer, E. Beyne, C. Yu, 3D stacking using Cu—Cu direct bonding, 3D Systems Integration Conference (3DIC), IEEE International, IEEE 2011, pp. 1–4.
[12] Y. Hu, C. Liu, M. Lii, K. Rebibis, A. Jourdain, A. La Manna, E. Beyne, C. Yu, Cu—Cu hybrid bonding as option for 3D IC stacking, Interconnect Technology Conference (IITC), IEEE International, IEEE 2012, pp. 1–3.
[13] K. Hummler, B. Sapp, J.R. Lloyd, S. Kruger, S. Olson, S. Park, B. Murray, D. Jung, S.M. Cain, A.Y. Park, D. Ferrone, A. Imran, TSV and Cu—Cu direct bond wafer and package-level reliability, Electronic Components and Technology Conference (ECTC), IEEE 2013, pp. 41–48.
[14] K.H. Lu, X. Zhang, S.K. Ryu, J. Im, R. Huang, P.S. Ho, Thermo-mechanical reliability of 3-D ICs containing through silicon vias, Electronic Components and Technology Conference, IEEE 2009, pp. 630–634 ECTC 2009 59th.
[15] S. Park, H. Lee, B. Sammakia, K. Raghunathan, Predictive model for optimized design parameters in flip-chip packages and assemblies, IEEE Trans. Compon. Packag. Technol. 30 (2) (2007) 294–301.
[16] M.A. Hopcroft, W.D. Nix, T.W. Kenny, What is the Young's modulus of silicon? J. Microelectromech. Syst. 19 (2) (2010) 229–238.
[17] ANSYS Academic Research, 11.2. Solving Fracture Mechanics Problems, Released 14.0
[18] P.C. Paris, G.C. Sih, Stress Analysis of Cracks, 381, ASTM stp, 1965 30–83.
[19] A.Y. Park, S.C. Chaparala, S.B. Park, A fracture mechanics based parametric study with dimensional variables of the Cu-Cu direct thermo-Compression bonded interface using FEA, In Electronic Components and Technology Conference (ECTC) 2015, pp. 1926–1931 IEEE 65th.
[20] E.J. Jang, S. Hyun, H.J. Lee, Y.B. Park, Effect of wet pretreatment on interfacial adhesion energy of Cu—Cu thermocompression bond for 3D IC packages, J. Electron. Mater. 38 (12) (2009) 2449–2454.
[21] E.J. Jang, J.W. Kim, B. Kim, T. Matthias, Y.B. Park, Annealing temperature effect on the Cu—Cu bonding energy for 3D-IC integration, Met. Mater. Int. 17 (no. 1) (2011) 105–109.

Please cite this article as: A.-Y. Park, et al., Risk assessment of the crack propagation and delamination of the Cu-to-Cu direct bonded (CuDB) interface, Microelectronics Reliability (2016), http://dx.doi.org/10.1016/j.microrel.2016.09.015

[22] C.S. Tan, G.Y. Chong, High throughput Cu-Cu bonding by non-thermo-compression method, In Electronic Components and Technology Conference (ECTC) (2013) 1158–1164 IEEE 63rd.
[23] M.C. Hsieh, S.T. Wu, C.J. Wu, J.H. Lau, R.M. Tain, W.C. Lo, Energy release rate investigation for through silicon vias (TSVs) in 3D IC integration, In Thermal, Mechanical and Multi-Physics Simulation and Experiments in Microelectronics and Microsystems (EuroSimE) 2011, pp. 1–7 12th International Conference on.
[24] M.C. Hsieh, S.T. Wu, C.J. Wu, J.H. Lau, Energy release rate estimation for through silicon vias in 3-D IC integration, IEEE Trans. Compon. Packag. Manuf. Technol. 4 (1) (2014) 57–65.
[25] C.S. Selvanayagam, J.H. Lau, X. Zhang, S.K.W. Seah, K. Vaidyanathan, T.C. Chai, Nonlinear thermal stress/strain analyses of copper filled TSV (through silicon via) and their flip-chip microbumps, IEEE Trans. Adv. Packag. 32 (4) (2009) 720–728.
[26] D.P. Rooke, D.J. Cartwright, Compendium of stress intensity factors, Procurement Executive, Ministry of Defence. H. M. S. O, 1976 330.
[27] I.D. Parsons, J.F. Hall, A finite element investigation of the elastostatic state near a three dimensional edge crack, Eng. Fract. Mech. 33 (no. 1) (1989) 45–63.
[28] A. Zehnder, Linear elastic stress Analysis of 2D cracks, In Fracture Mechanics, Springer, Netherlands 2012, pp. 7–32.

Please cite this article as: A.-Y. Park, et al., Risk assessment of the crack propagation and delamination of the Cu-to-Cu direct bonded (CuDB) interface, Microelectronics Reliability (2016), http://dx.doi.org/10.1016/j.microrel.2016.09.015